

See discussions, stats, and author profiles for this publication at: <https://www.researchgate.net/publication/322895470>

# Non-enzymatic glucose sensing platform using self assembled cobalt oxide/graphene nanocomposites immobilized graphite modified electrode

Article in *Journal of Materials Science: Materials in Electronics* · April 2018

DOI: 10.1007/s10854-018-8662-7

CITATIONS

14

READS

190

5 authors, including:



**Suresh Babu Rajendran**

Centro Federal de Educação Tecnológica Celso Suckow da Fonseca (CEFET/RJ)

87 PUBLICATIONS 1,918 CITATIONS

[SEE PROFILE](#)



**Keshava Prasanna**

Channabasaveshwara Institute of Technology

25 PUBLICATIONS 333 CITATIONS

[SEE PROFILE](#)



**Chang Woo Lee**

Kyung Hee University

553 PUBLICATIONS 12,750 CITATIONS

[SEE PROFILE](#)



# Non-enzymatic glucose sensing platform using self assembled cobalt oxide/graphene nanocomposites immobilized graphite modified electrode

R. Vivekananth<sup>1</sup> · R. Suresh Babu<sup>1</sup> · K. Prasanna<sup>2,3</sup> · Chang Woo Lee<sup>2</sup> · R. A. Kalaivani<sup>1</sup>

Received: 18 September 2017 / Accepted: 23 January 2018  
© Springer Science+Business Media, LLC, part of Springer Nature 2018

## Abstract

A new strategy to prepare the densely packed cobalt oxide (Co<sub>3</sub>O<sub>4</sub>)/graphene nanocomposites by a self-assembly method were adopted in this work. A new non-enzymatic glucose determination has been fabricated by using Co<sub>3</sub>O<sub>4</sub>/graphene nanocomposites modified electrode as a sensing material. The nanocomposites were characterized using X-ray diffraction, X-ray photoelectron spectroscopy and field emission scanning electron microscopy, which confirms the successful formation of dense packed Co<sub>3</sub>O<sub>4</sub>/graphene nanocomposite. The results of Co<sub>3</sub>O<sub>4</sub>/graphene nanocomposites modified electrode exhibit good electrocatalytic activity toward the oxidation of glucose in 0.1 M NaOH by cyclic voltammetry. Under optimal conditions, the oxidation peak current was proportional to the glucose concentration in the range from 16.0 μM to 1.3 mM with a detection limit of 0.5 μM. The determination of glucose with the modified electrode shows the advantages of ease of preparation, high sensitivity and good stability. The analytical utility of the modified electrode as an amperometric sensor for the determination of glucose in the flow systems was evaluated by chronoamperometric studies. The practical application of the modified electrode for glucose determination has been evaluated in urine samples.

## 1 Introduction

In recent years, nanoscale devices have attracted significant attention because of their superior performances as they exhibit unique properties which differ from the bulk properties. A wide variety of nanomaterials with different sizes, shapes and compositions are now available [1]. The huge interest in nanomaterials is driven by their many desirable properties. The ability to tailor the size and structure and the properties of nanomaterials offer excellent prospects

for designing novel sensing systems and enhancing the performance of the bioanalytical assay. Diabetes mellitus is a worldwide health care problem that seriously affects normal life of people [2]. Blood glucose level is a basic issue in the diagnosis and treatment of diabetes. Hence, there is a great demand for the development of glucose biosensor which can reliably and rapidly monitor the level of glucose in clinical diagnostics [3]. The conventional glucose oxidase (GOx) enzyme modified electrode is the most common class of amperometric biosensors for glucose detection because GOx enables catalytic oxidation of glucose with high sensitivity and selectivity [4, 5]. However, the GOx-based biosensors have several disadvantages, such as instability, high cost and complicated fabrication [6, 7]. Recently, it has been recognized that non-enzymatic glucose electrochemical sensors can offer a unique set of physical and practical properties that may be exploited in glucose detection as an alternative to the use of GOx-based biosensors.

Non-enzymatic glucose sensors were developed by various nanomaterials modified electrodes like precious metals and their alloys (Au, Pt, Pd, Pt–Au, Pt–Pd) [8, 9] transition metals and their oxides (Ni, Cu, CuO, NiO, CoO, Co<sub>3</sub>O<sub>4</sub>) [10–20] and transition metal complexes [21]. Amongst these materials, Co<sub>3</sub>O<sub>4</sub> nanoparticles have demonstrated

✉ Chang Woo Lee  
cwlee@khu.ac.kr

✉ R. A. Kalaivani  
rakvani@yahoo.co.in

<sup>1</sup> Department of Chemistry, School of Basic Sciences, Vels University, Pallavaram, Chennai, Tamil Nadu 600 117, India

<sup>2</sup> Department of Chemical Engineering, Center for the SMART Energy Platform, College of Engineering, Kyung Hee University, 1732 Deogyong-daero, Gihung, Yongin, Gyeonggi 17104, South Korea

<sup>3</sup> Department of Energy Conversion and Storage, Technical University of Denmark, Frederiksborgvej 399, P.O. Box 49, 4000 Roskilde, Denmark

to be the promising material for non-enzymatic glucose sensor, supercapacitor, lithium ion battery, gas sensing and solar cells due to its low cost, good redox activity, environment friendly and relatively good conductivity. These nanomaterials can easily lose their shelf-life due to its aggregation and loss of their structural integrity by pulverization and the deterioration of the nanostructure. Hence, the modified electrode needs to keep maintain the size and structure of the nanomaterials without any passivation from electrode surface.

Graphene as a well known one atom thick two-dimensional graphitic carbon nanostructure with a single layer of carbon atoms densely packed in a honeycomb lattice. It has been utilized to be an efficient modified electrode material for electrochemical and biosensors in recent years, due to its superior electrical conductivity, mechanical properties, high surface-to-volume ratio, ultrathin thickness, structural flexibility, and chemical stability [22]. Meanwhile, graphene based modified electrodes showed good sensitivity, selectivity and stability towards for the electrochemical determination of biomolecules and glucose [23, 24]. These extraordinary features prompt the application of graphene and support to synthesize graphene based metal oxide nanocomposite hybrids for electrochemical determination of non enzymatic and enzymatic glucose sensors. To load a large number of metal oxides nanoparticles, graphene was usually functionalized by some organic molecules based on physical absorption or covalent immobilization [25]. However, the poor immobilization usually resulted in leaching off metal oxides from the nanosheet during electrochemical analysis. Consequently, the prepared modified electrodes suffer from poor reproducibility, thermal, mechanical and chemical instability, regardless of high sensitivity and low detection limit. Therefore, more efforts are still needed to design novel metal oxide/graphene nanocomposites for developing reliable electrochemical glucose sensor.

Combining the advantageous features of self assembled graphene stacks and  $\text{Co}_3\text{O}_4$  nanoparticles,  $\text{Co}_3\text{O}_4$ /graphene nanocomposite modified electrode has been successfully constructed and used for the non-enzymatic glucose sensor. The structure and morphology  $\text{Co}_3\text{O}_4$ /graphene nanocomposite were confirmed using X-ray diffraction (XRD) and FESEM. The electrochemical property of the modified electrode was evaluated through cyclic voltammetry and electrochemical impedance spectroscopy. The  $\text{Co}_3\text{O}_4$ /graphene nanocomposite modified electrode exhibits a good electrocatalytic activity toward the oxidation of glucose with high sensitivity and remarkable stability in static and dynamic conditions. The practical utility of the modified electrode was also evaluated for the determination of glucose in urine samples.

## 2 Experimental

### 2.1 Instrumentation

Electrochemical measurements were performed in a conventional three-electrode electrochemical cell using CHI 760D electrochemical workstation (CH Instruments, USA) controlled by a personnel computer. A platinum wire and a saturated calomel electrode (SCE) were used as auxiliary and reference electrodes, respectively. The  $\text{Co}_3\text{O}_4$ /graphene nanocomposite modified electrode employed as the working electrode was prepared according to the procedure described below. A magnetic Teflon stirrer was provided for the convective transport during the amperometric measurements. All experiments were performed at ambient temperature. XRD analysis was performed using Bruker model D8 with  $\text{Cu K}\alpha$  radiation. Field emission scanning electron microscope (FE-SEM) and energy dispersive X-ray spectroscopy (EDS) data were obtained using a SU6600, HITACHI, Japan, equipped with an EDS analyzer at an accelerating voltage of 30 kV.

### 2.2 Synthesis of the $\text{Co}_3\text{O}_4$ /graphene nanocomposite

The synthesis of the  $\text{Co}_3\text{O}_4$ /graphene nanocomposite was carried out using a slightly modified procedure with an earlier report [25]. For the synthesis of graphene amine, graphene oxide (300 mg) was dispersed in aqueous solution (200 mL) by ultrasonicator for 1 h. Hexamethylene diamine (0.01 mol) in 100 mL aqueous solution is slowly added into the graphene oxide solution and stirred continuously for 48 h. The resultant precipitate was collected, washed with anhydrous ethanol and dried in a vacuum oven (50 °C) for 24 h.

For the synthesis of  $\text{Co}_3\text{O}_4$ /graphene nanocomposite, graphene oxide (50 mg) was dispersed in water (100 mL) by pulse sonication. An aqueous solution of cobalt chloride (0.20 M, 14 mL) was added dropwise into the graphene oxide solution and was stirred for 15 min. Graphene amine (50 mg) was dispersed to the mixed solution containing ethanol (150 mL) and water (150 mL). Finally, graphene amine is slowly added to graphene oxide/cobalt chloride solution and stirred for 15 min, and with 1 equivalent of NaOH was slowly added to the above solution until the pH reaches 12. Finally  $\text{H}_2\text{O}_2$  aqueous solution (8 mL, 1 wt%) were added dropwise to the above solution. Then the mixture was heated at 120 °C for 16 h. Then, the precipitate was washed with anhydrous ethanol and dried overnight at 60 °C in conventional oven. The  $\text{Co}_3\text{O}_4$ /graphene nanocomposite was ground and reduced at 400 °C in

a flow of Ar gas for 2 h. The schematic illustrations showing the preparation of  $\text{Co}_3\text{O}_4$ /graphene nanocomposites and electrocatalytic activity is shown in Scheme 1.

### 2.3 Fabrication of the $\text{Co}_3\text{O}_4$ /graphene nanocomposite modified electrode

Before modification, the wax impregnated graphite electrode was prepared using an earlier reports [26, 27] by heating the spectroscopic grade graphite rods (0.3 cm circular diameter, 4.0 cm length) in molten wax with the application of suction for 30 min, until air bubbles ceased to evolve from the rods. After re-establishing the atmospheric pressure, the rods were removed before the paraffin solidified. The lower end of the electrode was polished using various grades of emery sheets with a fine mirror polish was obtained for surface modification of the electrode. The polished surface was then washed with methanol and distilled water. For surface modification, 1 mg of  $\text{Co}_3\text{O}_4$ /graphene nanocomposite was suspended in 1 mL of ethanol containing 1% Nafion solution and sonicated for 30 min. Then 10  $\mu\text{L}$  of the suspension was cast on the polished paraffin impregnated graphite electrode surface and dried in air. The resulted  $\text{Co}_3\text{O}_4$ /graphene nanocomposite electrode was stored in air-tight container at room temperature.

## 3 Results and discussion

### 3.1 XRD and XPS of $\text{Co}_3\text{O}_4$ /graphene nanocomposite

The crystal structure formation of  $\text{Co}_3\text{O}_4$ /graphene nanocomposites was confirmed by XRD. Figure 1a shows the XRD patterns of  $\text{Co}_3\text{O}_4$ /graphene nanocomposites and

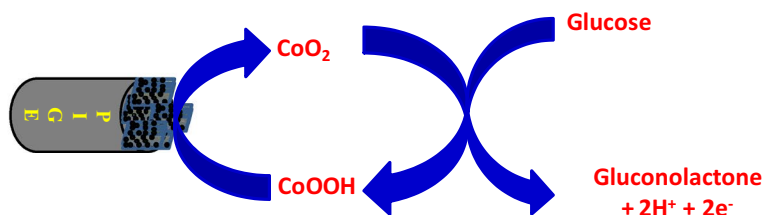
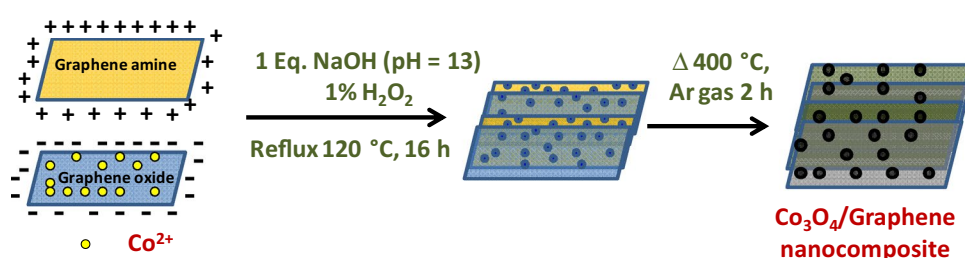
commercial  $\text{Co}_3\text{O}_4$  (for comparison). For  $\text{Co}_3\text{O}_4$  nanoparticles, the  $2\theta$  values of  $19.0^\circ$ ,  $31.2^\circ$ ,  $36.8^\circ$ ,  $38.5^\circ$ ,  $44.8^\circ$ ,  $49.0^\circ$ ,  $55.6^\circ$ ,  $59.3^\circ$  and  $65.2^\circ$  were clearly distinguishable, indicates the nanocomposite was phase pure. The peak positions are in good agreement of  $\text{Co}_3\text{O}_4$  (space group  $Fd-3m$  JCPDS No. 01-073-1701). It demonstrates the as prepared nanocomposite is cubic crystal of  $\text{Co}_3\text{O}_4$ . For reference, the XRD pattern of commercial  $\text{Co}_3\text{O}_4$  also displayed in Fig. 1a. The XRD pattern of commercial  $\text{Co}_3\text{O}_4$  and  $\text{Co}_3\text{O}_4$ /graphene nanocomposites showed same characteristics, confirming the formation of  $\text{Co}_3\text{O}_4$ . The average crystalline size was determined from the half width of the diffraction peaks using the Debye–Scherrer formula and was found to be approximately 15 nm. Further, broad diffraction broad peaks of  $2\theta$  between  $19^\circ$  and  $27^\circ$  correspond to the graphitic domains of the graphene stacks.

To further confirm the presence of  $\text{Co}_3\text{O}_4$  in graphene nanocomposites, X-ray photoelectron spectroscopy (XPS) measurements were carried out. High resolution XPS peaks on Co (2p), the binding energies are located at 780.18 and 795.28 eV with correspond to Co  $2p_{3/2}$  and Co  $2p_{1/2}$  of  $\text{Co}_3\text{O}_4$ , respectively, as shown in Fig. 1b. These observations are consistent with earlier reports [28].

### 3.2 FESEM images of $\text{Co}_3\text{O}_4$ /graphene nanocomposite

The structure and morphology of the  $\text{Co}_3\text{O}_4$ /graphene nanocomposite were characterized using FESEM as shown in Fig. 2a. It can be seen that, the edges of the graphene sheets were corrugated and densely aligned with few millimeters thick and the graphene sheets interconnected with  $\text{Co}_3\text{O}_4$  nanoparticles inside. No significant aggregation of  $\text{Co}_3\text{O}_4$  and graphene was observed in the morphology, indicating that the graphene were

**Scheme 1** Schematic illustration of the fabrication of  $\text{Co}_3\text{O}_4$ /graphene nanocomposite and electrocatalytic oxidation mechanism of glucose at the modified electrode



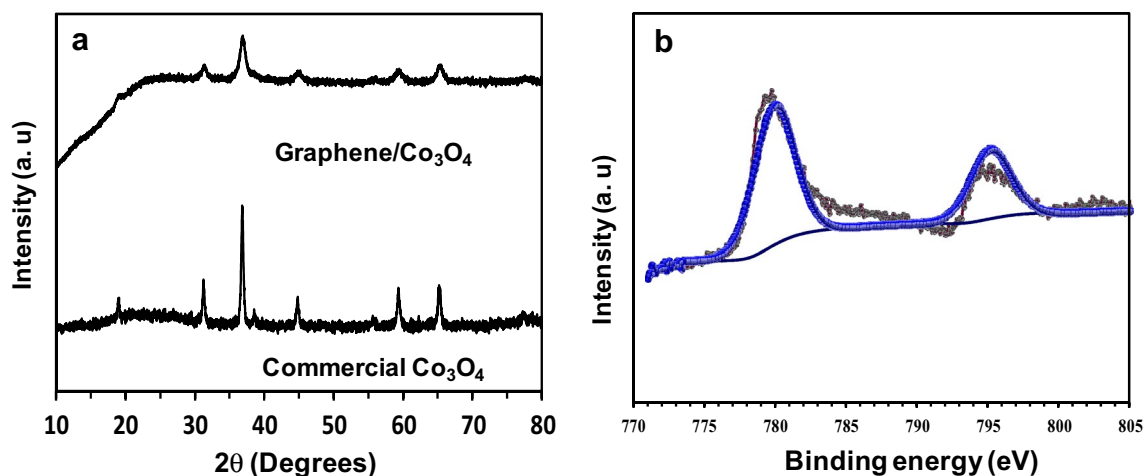


**Fig. 1** **a** XRD pattern of commercial  $\text{Co}_3\text{O}_4$  and  $\text{Co}_3\text{O}_4$ /graphene nanocomposite. **b** High resolution XPS spectrum for Co 2p core regions of  $\text{Co}_3\text{O}_4$ /graphene nanocomposite

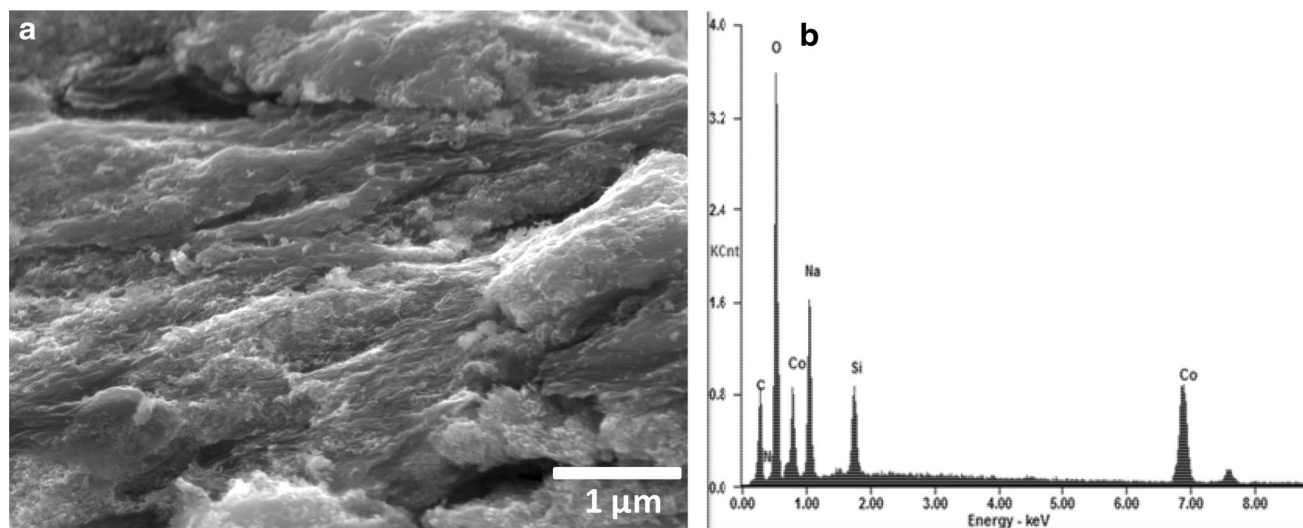


**Fig. 2** **a** FESEM image and **b** EDS spectrum of  $\text{Co}_3\text{O}_4$ /graphene nanocomposite

alternatively packed inside of  $\text{Co}_3\text{O}_4$  nanoparticles. The average diameter of these  $\text{Co}_3\text{O}_4$  particles was about  $\sim 15\text{--}20$  nm. These morphology results the  $\text{Co}_3\text{O}_4$  is strongly packed in graphene layers, it cannot be easily come out from the graphene stacks. Hence the  $\text{Co}_3\text{O}_4$ /graphene nanocomposite modified electrode has excellent stability towards glucose oxidation. In order to confirm that  $\text{Co}_3\text{O}_4$  has successfully sandwiched inside the graphene layers, EDS analysis was also evaluated. Figure 2b shows the EDS spectra for  $\text{Co}_3\text{O}_4$ /graphene nanocomposite of the elements of Co, O, and C are obviously observed.

### 3.3 Electrochemical behavior of $\text{Co}_3\text{O}_4$ /graphene nanocomposite modified electrode

The electrochemical behavior of  $\text{Co}_3\text{O}_4$ /graphene nanocomposite modified electrode was studied by cyclic voltammetry. Cyclic voltammetric investigations of the  $\text{Co}_3\text{O}_4$ /graphene nanocomposite modified electrode reveals (Fig. 3) two pairs of well-defined redox peaks corresponding to the immobilized  $\text{Co}_3\text{O}_4$ /graphene nanocomposite when the potential was swept in the range from  $-0.2$  to  $0.6$  V at a scan rate of  $20$  mV/s in  $0.1$  M NaOH (curve b). The bare electrode under similar condition does not

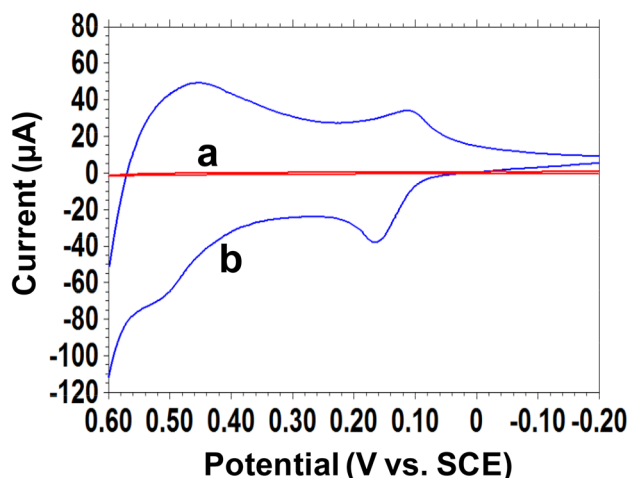
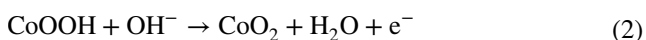


**Fig. 3** Cyclic voltammograms of the (a) bare electrode and (b)  $\text{Co}_3\text{O}_4$ /graphene nanocomposite modified electrode in 0.1 M NaOH at the scan rate of 20 mV/s

show any characteristic wave (curve a).  $\text{Co}_3\text{O}_4$ /graphene nanocomposite modified electrode exhibited a first anodic peak at +0.20 V and a cathodic peak at +0.11 V attributed to conversion of  $\text{Co}_3\text{O}_4$  and  $\text{CoOOH}$  and second anodic peak at +0.52 V and a cathodic peak at +0.47 V can be assigned to the transition between  $\text{CoOOH}$  and  $\text{CoO}_2$ . These redox reactions suggesting that hydroxyl ion participates in the electrochemical redox reaction of  $\text{Co}_3\text{O}_4$ . According to this result, it seems that the electrochemical behavior of the  $\text{Co}_3\text{O}_4$ /graphene nanocomposite modified electrode in alkaline solution is similar to that of  $\text{Co}_3\text{O}_4$ /MWNT [13] and nanoporous  $\text{Co}_3\text{O}_4$  [14] alloy electrode in the alkaline solution. This possible mechanism with two redox reactions can be represented in the following reactions [28].



The impedance changes occurring at the electrode–electrolyte interfaces can be known by EIS. Figure 4 shows the Nyquist plots of bare and  $\text{Co}_3\text{O}_4$ /graphene nanocomposite modified electrode. The Nyquist plot shows a semicircle in high frequency corresponds to the interfacial charge transfer resistance ( $R_{ct}$ ), which is the most directive and sensitive factor showing the changes at the electrode–electrolyte interfaces. It can be seen that, the bare electrode (curve a) exhibits the largest  $R_{ct}$  (9557  $\Omega$ ), and it might be attributed to the wax impregnated graphite electrode surface acting as a barrier for the electrochemical process and hindering the access of the redox probe,  $[\text{Fe}(\text{CN})_6]^{3-/4-}$ , to the electrode surface [29]. Compared with bare electrode,  $R_{ct}$  is greatly decreased (190  $\Omega$ ) at the

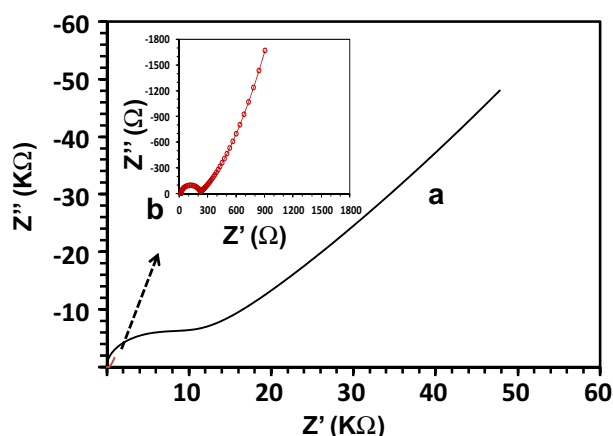
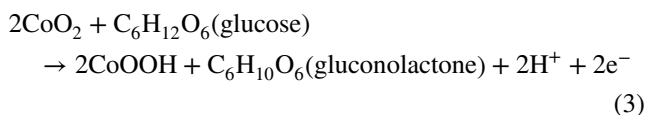


**Fig. 4** EIS of bare and  $\text{Co}_3\text{O}_4$ /graphene nanocomposite modified electrode in 5 mM  $\text{K}_4[\text{Fe}(\text{CN})_6]$  in 0.1 M KCl solution, with the frequency swept from 1 Hz to 0.1 MHz. Inset: enlarged view of  $\text{Co}_3\text{O}_4$ /graphene nanocomposite modified electrode

$\text{Co}_3\text{O}_4$ /graphene nanocomposite modified electrode (curve b) due to the excellent electrical conductivity of  $\text{Co}_3\text{O}_4$ /graphene nanocomposite.

### 3.4 Electrocatalytic oxidation of glucose

Figure 5a shows the cyclic voltammograms of the  $\text{Co}_3\text{O}_4$ /graphene nanocomposite modified electrode in the presence of various concentrations of glucose. The catalytic current for glucose oxidation showed corresponding linearity in the concentration range of 16.0  $\mu\text{M}$  to 1.3 mM. The linear regression equation is expressed as  $I_{\text{pcat}} (\mu\text{A}) = 0.2708x + 6.3151$ ,  $[\text{glucose}]/(\mu\text{M})$  with correlation coefficient  $R^2 = 0.9909$  (Fig. 5b). The detection limit for glucose determination was found to be 0.51  $\mu\text{M}$ . The mechanism of electrocatalytic oxidation of glucose at the modified electrode is shown in Eq. (3):



The cyclic voltammogram for the bare electrode and with addition of 1.3 mM of glucose to 0.1 M NaOH is shown in the inset of Fig. 5a. The response obtained for glucose oxidation at a bare electrode is very poor when compared to the modified electrode. When the  $\text{Co}_3\text{O}_4$ /graphene nanocomposite modified electrode was used for oxidation compared to the bare electrode and the current response is also increased almost ten-fold, which makes the modified electrode as an effective sensor for glucose oxidation. The working potential, detection limit and linear concentration range of other related modified electrodes for glucose detection are reported in Table 1.

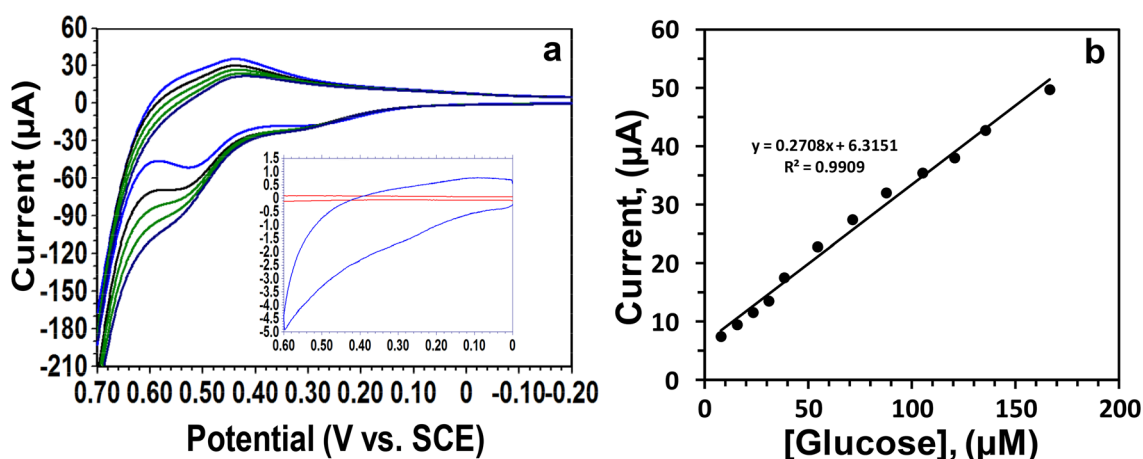


**Fig. 5 a** Cyclic voltammograms of  $\text{Co}_3\text{O}_4$ /graphene nanocomposite modified electrode in the absence and presence of 1 mM of glucose (inset) bare electrode in the absence and presence of 1 mM glucose in

0.1 M NaOH (scan rate 20 mV/s). **b** Calibration plot for the determination of glucose

**Table 1** Comparison of various nano metal oxide-based sensors for glucose detection with previous reports

Modified electrode	Fixed potential (V)	Electrolyte	Linear range ( $\mu\text{M}$ )	Detection limit ( $\mu\text{M}$ )	Ref.
$\text{Co}_3\text{O}_4$ nanoparticles/GCE	+0.59	0.1 M NaOH	5–800	0.1	[15]
NiO/Ni foam	+0.55	0.5 M NaOH	5–5500	0.4	[16]
CuO nanospheres	+0.60	0.1 M NaOH	Upto 2600	1.0	[17]
Functionalized NiNP	+0.55	0.1 KOH	1.6–1400	0.5	[11]
Functionalized CuNP	+0.35	0.1 M NaOH	6.6–1300	2.2	[12]
$\text{Co}_3\text{O}_4$ needle/graphene	+0.60	0.1 M NaOH	50–300	< 10	[18]
$\text{Co}_3\text{O}_4$ /graphene	+0.58	0.1 M NaOH	Upto 80	0.025	[19]
$\text{Co}_3\text{O}_4$ /GO hydrogel	+0.62	0.1 M NaOH	250–10,000	250	[20]
$\text{Co}_3\text{O}_4$ /graphene nanocomposite	+0.58	0.1 M NaOH	16–1300	0.5	This work

### 3.5 Amperometry

Linear sweep voltammetric (LSV) studies were carried out in order to evaluate the influence of flow conditions on the catalytic oxidation of glucose as a function of the applied potential. LSVs of bare electrode and the modified electrode obtained in presence of 440  $\mu\text{M}$  of glucose in a stirring solution of 0.1 M NaOH at the scan rate of 20 mV/s (Fig. not shown). The electrocatalytic activity of the modified electrode permitted the convenient detection of glucose at lower potentials with high sensitivity when compared to the bare electrode. In the presence of glucose, the current response increases from +0.40 V, reaching a maximum value at +0.55 V with a sigmoidal shape. This behavior illustrates that the oxidation of glucose is greatly enhanced at the modified electrode due to the electrocatalysis. Hence, a potential of +0.58 V was selected as the working potential for amperometric determination of glucose using modified electrode under hydrodynamic conditions.

The amperometric response of the  $\text{Co}_3\text{O}_4$ /graphene nanocomposite modified electrode for the electrocatalytic oxidation of glucose was carried out. The current–time response obtained for the modified electrode in a stirred solution (300 rpm) for successive increments of 0.5 mL of 1 mM glucose is shown in Fig. 6a (curve B). The same amount of concentration of glucose toward bare electrode also tested (curve A), which shows a very poor amperometric response was observed. The step-wise current response increases for increasing concentrations of glucose. The plot of catalytic current vs. glucose concentration is shown in Fig. 6b. A good linear response was obtained over the low range from 8.2  $\mu\text{M}$  to 76  $\mu\text{M}$  glucose with a slope of 0.175  $\mu\text{A}/\mu\text{M}$  (sensitivity) and a correlation coefficient of 0.9913 for the part of the shown amperogram. High sensitivity can be attributed to the synergistic augmentation of densely packed graphene and  $\text{Co}_3\text{O}_4$  nanocomposite towards glucose oxidation. Such a good response of the

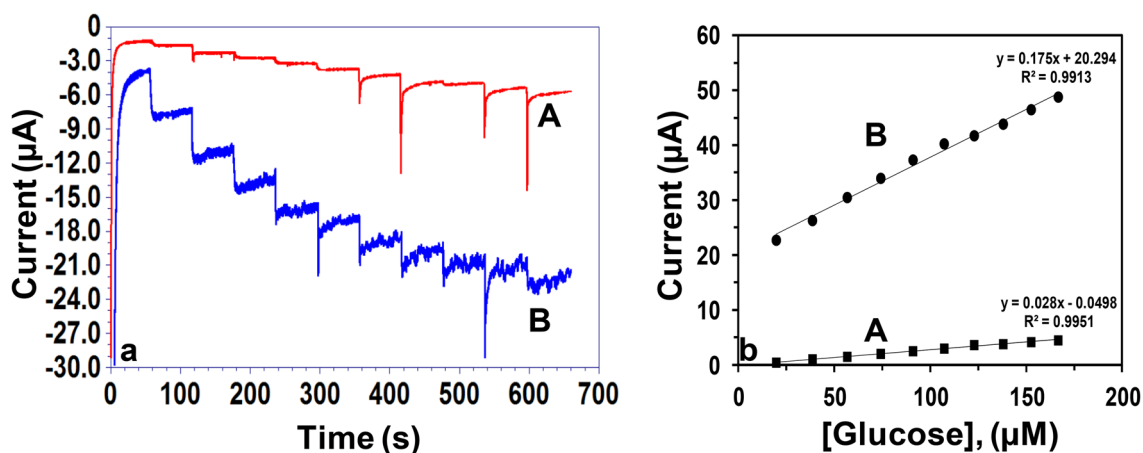


**Fig. 6** a Typical amperometric current response of the (A) bare and (B)  $\text{Co}_3\text{O}_4/\text{graphene}$  nanocomposite modified electrode and upon the successive injection of 0.5 mL of 1 mM glucose in to 0.1 M NaOH. b Calibration plot for the determination of glucose

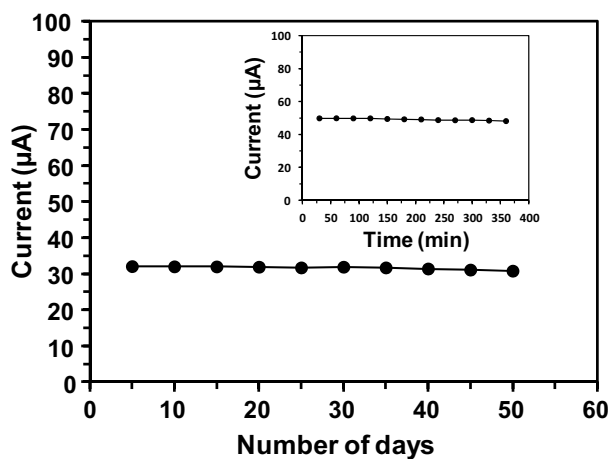


**Fig. 7** Long term stability response of the  $\text{Co}_3\text{O}_4/\text{graphene}$  nanocomposite modified electrode towards the oxidation of 82  $\mu\text{M}$  glucose. Inset: current response of  $\text{Co}_3\text{O}_4/\text{graphene}$  nanocomposite modified electrode towards the sensing of 162  $\mu\text{M}$  glucose under dynamic conditions for 6 h

modified electrode for oxidation of glucose under dynamic conditions justifies its feasible application in flow systems.

### 3.6 Stability

The shelf-time of the  $\text{Co}_3\text{O}_4/\text{graphene}$  nanocomposite modified electrode for the oxidation of glucose was monitored by recording the anodic current response at an interval of 5 days for 82  $\mu\text{M}$  glucose over a period of 60 days. The modified electrode suffered a current loss of 5.6% at the end of the 60 days showing that the modified electrode was appreciably stable for glucose determination as shown in Fig. 7. The long-term response of the modified electrode was checked by recording the anodic current for

**Table 2** Determination of glucose in urine samples (n=3)

Urine samples	Spiked ( $\mu\text{M}$ )	Found <sup>a</sup> ( $\mu\text{M}$ )	Recovery (%)
Sample 1	25	$26.1 \pm 0.4$	104.4
	50	$52.4 \pm 0.4$	104.8
Sample 2	25	$25.6 \pm 0.4$	102.4
	50	$51.8 \pm 0.4$	103.6

<sup>a</sup>Average of three measurements

the oxidation of 163  $\mu\text{M}$  glucose for every 30 min over an extended period of 6 h and almost a constant response was obtained as shown in inset of Fig. 7. It can be noticed from the Fig. 7, the modified electrode exhibits almost constant response suggesting the stable electrocatalytic oxidation toward glucose determination due to the  $\text{Co}_3\text{O}_4$  nanoparticles which has strongly interconnected densely within the graphene layers.

### 3.7 Real sample analysis

In order to study the analytical performance of  $\text{Co}_3\text{O}_4/\text{graphene}$  nanocomposite modified electrode towards glucose determination, the modified electrode was applied to the direct analysis of urine samples. As shown in Table 2, two human urine samples were analyzed for glucose determination. In order to fit into the linear range, all the samples used for detection were diluted to 100 times with 0.1 M NaOH without any treatment. The dilution can actually help in reducing the matrix effect of real samples. To ascertain the correctness of the results, the samples were spiked with certain amounts of glucose was detected. The recovery rates of the spiked samples were found between 102.4 and 104.8%.



## 4 Conclusions

In summary, a new strategy to prepare the densely packed cobalt oxide (Co<sub>3</sub>O<sub>4</sub>)/graphene nanocomposites by a self-assembly method and its application in non-enzymatic glucose sensor was fabricated. The Co<sub>3</sub>O<sub>4</sub>/graphene nanocomposite modified electrode displayed substantially higher electrocatalytic activity and faster response to glucose oxidation with a higher current response than conventional bare electrode. This Co<sub>3</sub>O<sub>4</sub>/graphene nanocomposite modified electrode based electrochemical sensor has a low detection limit of 0.5 μM and a very high sensitivity of 0.2708 μA/μM, and its response is linear from 16.0 μM to 1.3 mM glucose concentration. On comparison with the self assembled densely packed Co<sub>3</sub>O<sub>4</sub>/graphene nanocomposite, the modified electrode has superior electrochemical performance characteristics combined with long-term stability and good reproducibility.

**Acknowledgements** The authors gratefully acknowledge financial support from Defence Research and Development Organization (DRDO), New Delhi and also Vels University, Chennai, for providing infrastructure facilities.

## References

1. K. Miyazaki, N. Islam, *Technovation* **27**, 661–675 (2007)
2. P. Hossain, B. Kavar, M.E. Nahas, *N. Engl. J. Med.* **356**, 213–215 (2007)
3. G.S. Wilson, R. Gifford, *Biosens. Bioelectron.* **20**, 2388–2403 (2005)
4. S.G. Wang, Q. Zhang, R. Wang, S.F. Yoon, J. Ahn, D.J. Yang, J.Z. Tian, J.Q. Li, Q. Zhou, *Electrochem. Commun.* **5**, 800–803 (2003)
5. Y. Zou, C. Xiang, L.-X. Sun, F. Xu, *Biosens. Bioelectron.* **23**, 1010–1016 (2008)
6. R. Wilson, A.P.F. Turner, *Biosens. Bioelectron.* **7**, 165–185 (1992)
7. Y. Zhu, H. Zhu, X. Yang, L. Xu, C. Li, *Electroanalysis* **19**, 698–703 (2007)
8. K. Tian, M. Prestgard, A. Tiwari, *Mater. Sci. Eng. C* **41**, 100–118 (2014)
9. Y. Sun, H. Buck, T.E. Mallouk, *Anal. Chem.* **73**, 1599–1604 (2001)
10. X. Niu, X. Li, J. Pan, Y. He, F. Qiu, Y. Yan, *RSC Adv.* **6**, 84893–84905 (2016)
11. R.S. Babu, P. Prabhu, S.S. Narayanan, *Talanta* **110**, 135–143 (2013)
12. R.S. Babu, P. Prabhu, S.S. Narayanan, *RSC Adv.* **4**, 47497–47504 (2014)
13. R. Prasad, B.R. Bhat, *New J. Chem.* **39**, 9735–9742 (2015)
14. M. Zheng, L. Li, P. Gu, Z. Lin, H. Xue, H. Pang, *Microchim. Acta* **184**, 943–949 (2017)
15. C.T. Hou, Q. Xu, L.N. Yin, X.Y. Hu, *Analyst* **137**, 5803–5808 (2012)
16. C. Guo, Y. Wang, Y. Zhao, C. Xu, *Anal. Methods* **5**, 1644–1647 (2013)
17. E. Reitz, W. Jia, M. Gentile, Y. Wang, Y. Lei, *Electroanalysis* **20**, 2482–2486 (2008)
18. X.W. Wang, X.C. Dong, Y.Q. Wen, C.M. Li, Q.H. Xiong, P. Chen, *Chem. Commun.* **48**, 6490–6492 (2012)
19. X.C. Dong, H. Xu, X.W. Wang, Y.X. Huang, M.B. Chan-Park, H. Zhang, L.H. Wang, W. Huang, P. Chen, *ACS Nano* **6**, 3206–3213 (2012)
20. L.T. Hoa, J.S. Chung, S.H. Hur, *Sens. Actuators B* **223**, 76–82 (2016)
21. M. Benjamin, D. Manoj, K. Thenmozhi, P.R. Bhagat, D. Saravanakumar, S. Senthilkumar, *Biosens. Bioelectron.* **91**, 380–387 (2017)
22. V. Singh, D. Joung, L. Zhai, S. Das, S.I. Khondaker, S. Seal, *Prog. Mater. Sci.* **56**, 1178–1271 (2011)
23. F. Chekin, S.K. Singh, A. Vasilescu, V.M. Dhavale, S. Kurungot, R. Boukherroub, S. Szunerits, *ACS Sens.* **1**, 1462–1470 (2016)
24. F. Tehrani, B. Bavarian, *Sci. Rep.* **6**, 27975 (2016)
25. S.J.R. Prabakar, R.S. Babu, M. Oh, M.S. Lah, S.C. Han, J. Jeong, M. Pyo, *J. Power Sources* **272**, 1037–1045 (2014)
26. F. Scholz, B. Lange, *Trends Anal. Chem.* **11**, 359–367 (1992)
27. R.S. Babu, P. Prabhu, S.S. Narayanan, *J. Solid State Electrochem.* **20**, 1575–1583 (2016)
28. Y. Ding, Y. Wang, L. Su, M. Bellagamba, H. Zhang, Y. Lei, *Biosens. Bioelectron.* **26**, 542–548 (2010)
29. R.S. Babu, P. Prabhu, S.S. Narayanan, *J. Nanosci. Nanotechnol.* **16**, 8711–8718 (2016)